# Supporting Information for Pore-Size Dominated Electrochemical Properties of Covalent Triazine Frameworks as Anode Materials for K-ion Batteries

Shu-Ying Li[a], Wen-Hao Li[b], Xing-Long Wu[a, b], Yuyang Tian[a], Jieyu Yue[c], and Guangshan Zhu*[a]

[a] Key Laboratory of Polyoxometalate Science of the Ministry of Education, Faculty of Chemistry, Northeast Normal University, Changchun 130024, P. R. China.

[b] Key Laboratory for UV Light-Emitting Materials and Technology of Ministry of Education, Northeast Normal University, Changchun, Jilin 130024, P. R. China.

[c] College of Chemistry, Key Laboratory of Molecular and Nano Probes, Ministry of Education, Shandong Normal University, Jinan 250014, P. R. China..

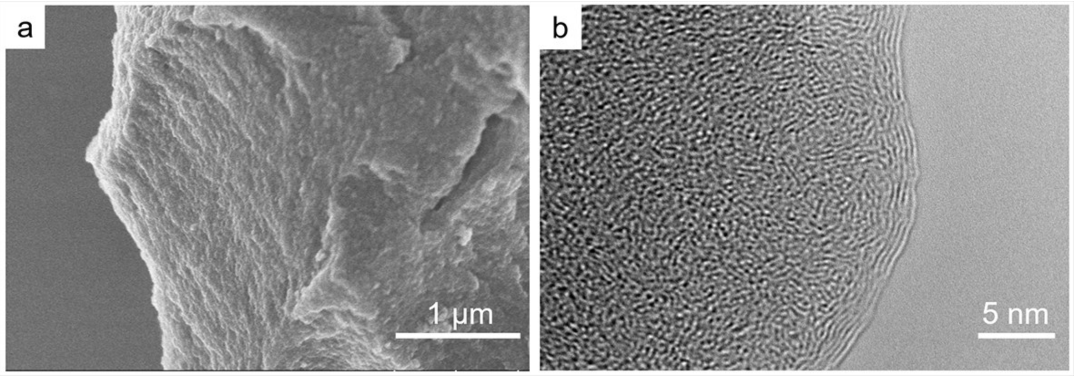

**Figure S1.** SEM image (a) and TEM image (b) of CTF-0.

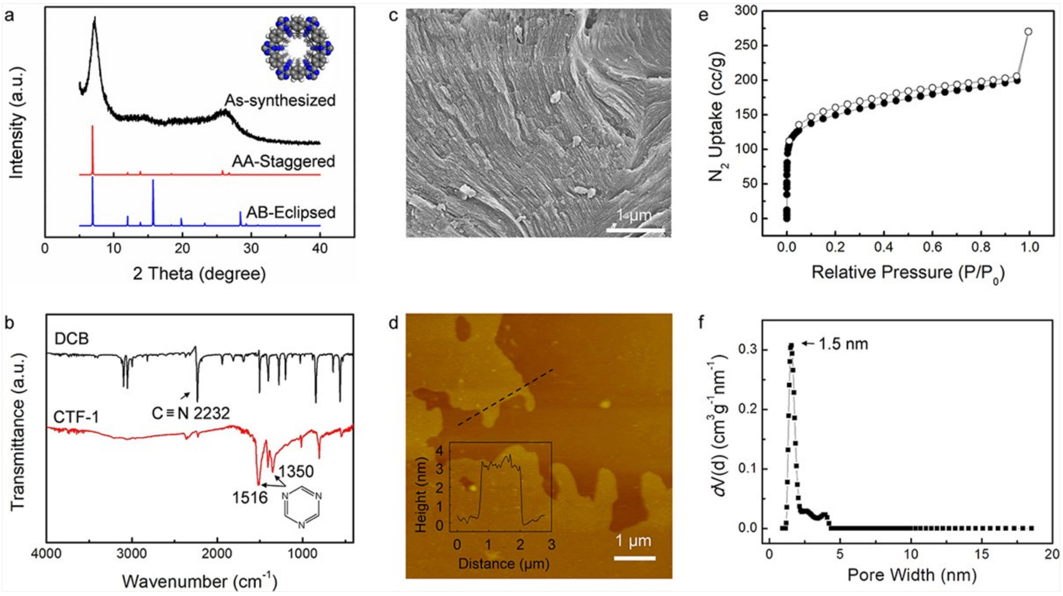

**Figure S2.** Morphology and structural characterizations of CTF-1. (a) PXRD patterns; (b) FT-IR spectra, DCB stands for the monomer *p*-dicyanobenzene; (c) SEM image; (d) AFM image of CTF-1 and height profile along the black line; (e) $N_2$ adsorption isotherms collected at 77 K. The relative pressure ($P/P_0$) range for determination of the CTF-1 BET surface area is from $9.0473\times10^{-3}$ to $9.9530\times10^{-2}$; (f) Pore size distribution of CTF-1.

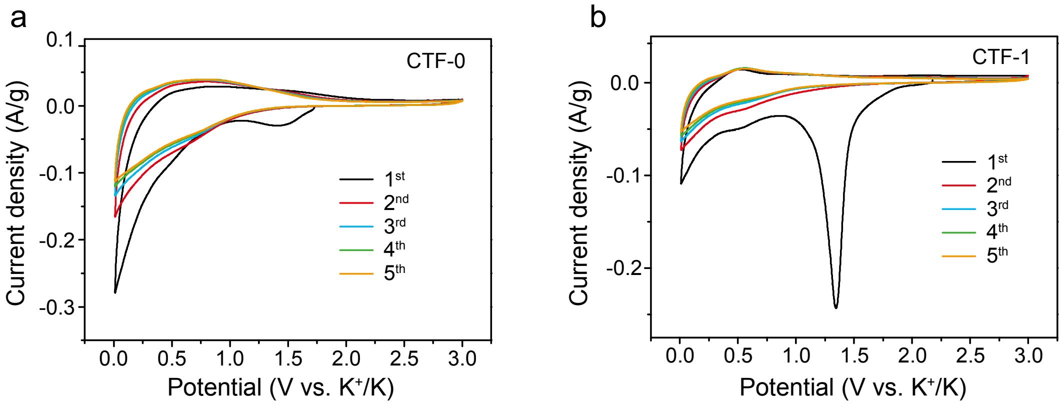

**Figure S3**. The cyclic voltammetry tests (CV) of the (a) CTF-0 and (b) CTF-1

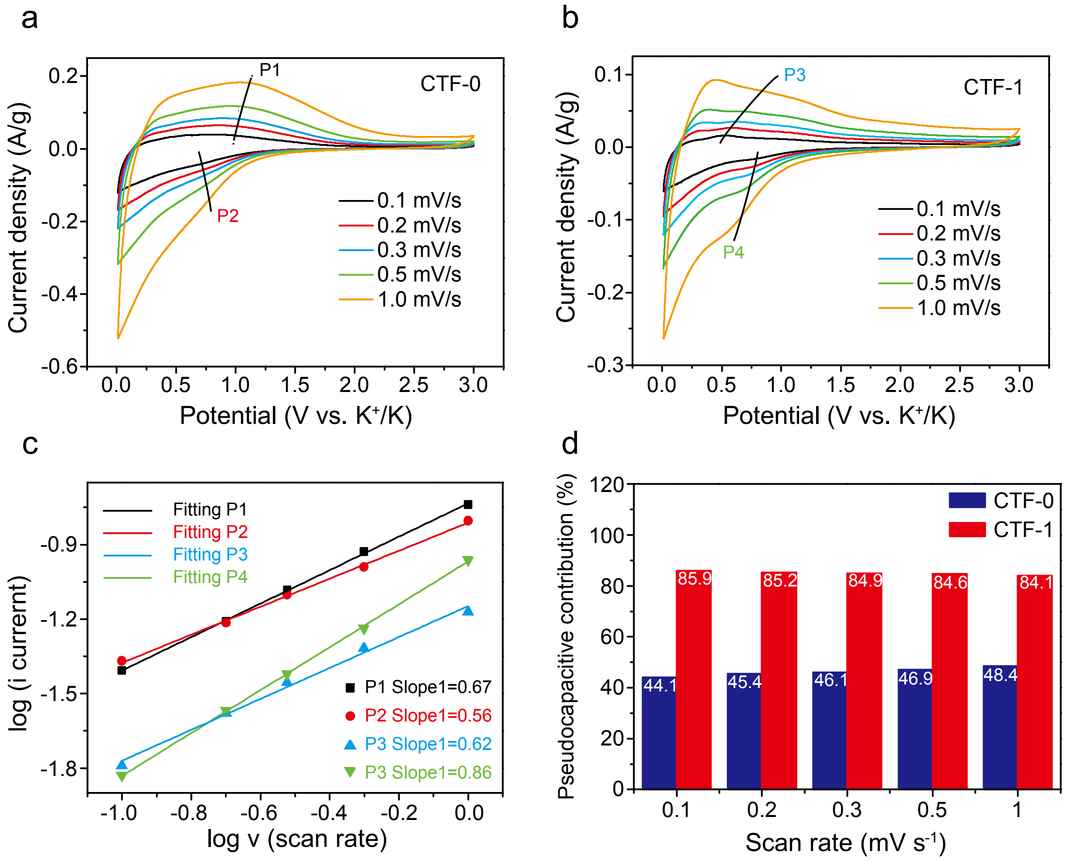

**Figure S4**. CV curves at different scan rates of (a) CTF-0 and (b) CTF-1; (c) log (i) vs log (*v*) plots for the CTF-0 and CTF-1; (d) pseudocapacitive contributions of CTF-0 and CTF-1 at different scan rates.

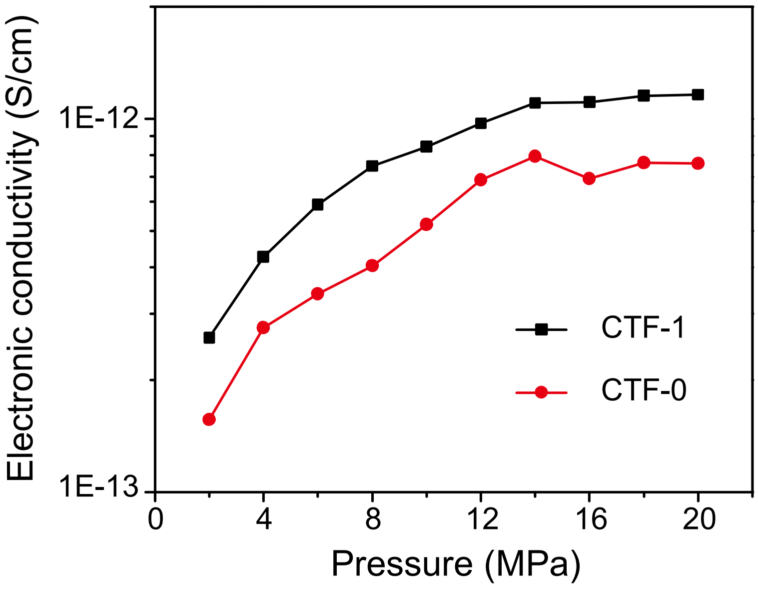

**Figure S5.** The electronic conductivity of CTFs under various pressures.

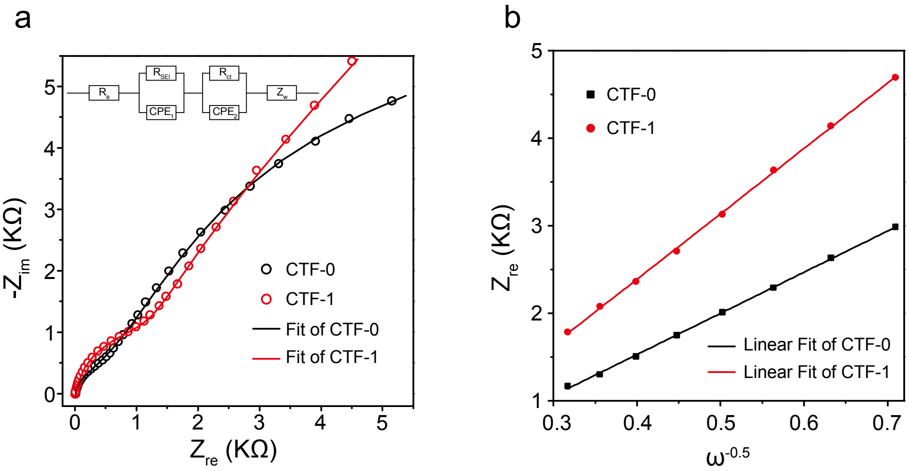

**Figure S6**. (a) Nyquist plots of electrochemical impedance spectroscopy (EIS) and the fitting for the CTF-0 and CTF-1 at open circuit after 50 cycles and the corresponding equivalent circuit. $R_e$, $R_{SEI}$, $R_{ct}$, $Z_w$ represent the resistant of electrolyte comprising all contacts, the resistant of SEI film, the charge transfer resistant and the Warburg resistance, respectively. (b) Dependence of $Z_{re}$ on the reciprocal square root of the frequency ($\omega^{-1/2}$) in the low-frequency region for CTF-0 and CFT-1.

**Table S1**. The comparison of EIS fitting results between the CTF-0 and CTF-1 after 50 cycles.

| **Samples** | **$R_e$ (Ω)** | **$R_{SEI}$ (Ω)** | **$R_{ct}$ (Ω)** |
|---|---|---|---|
| CTF-0 | 14.3 | 329.5 | 3368 |
| CTF-1 | 24.8 | 1216 | 2380 |

**Table S2**. The apparent potassium ion diffusion coefficient ($D_{app}$) calculated from the EIS of the CTFs.

| **Samples** | **Slope** | **$D_{app}$ ($\times 10^{-20}$ cm$^2$/s)** |
|---|---|---|
| CTF-0 | 4701.47 | 597.2 |
| CTF-1 | 7470.22 | 6.571 |

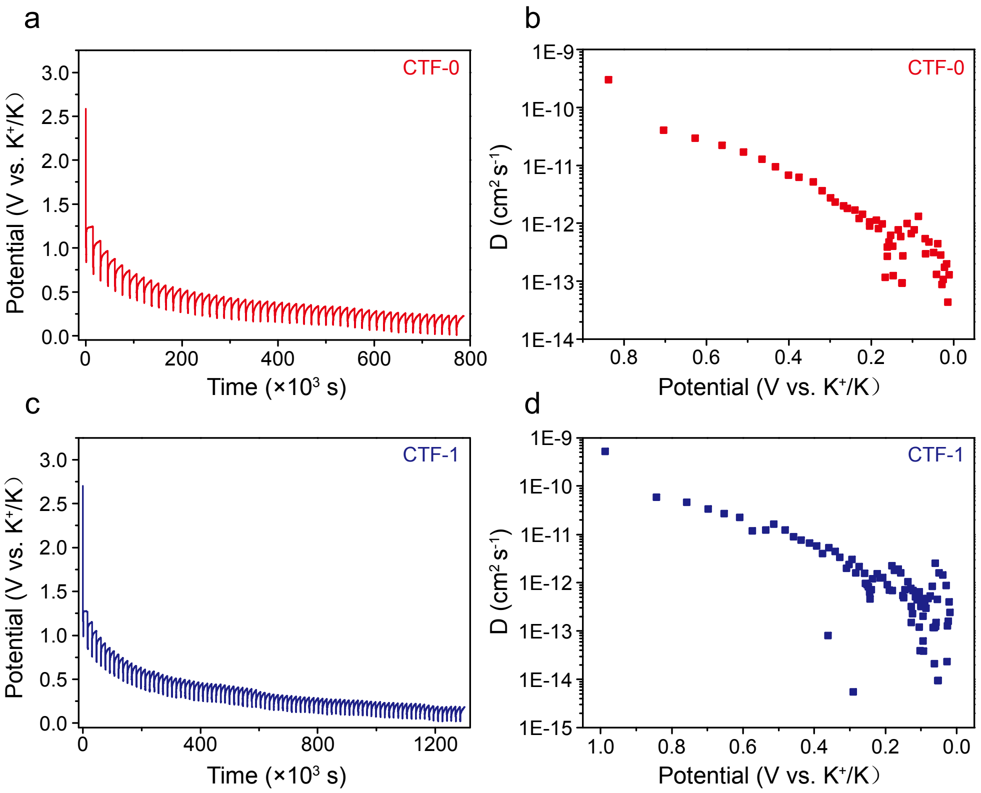

**Figure S7**. The galvanostatic intermittent titration technique (GITT) curves of (a) CTF-0 and (c) CTF-1 at the second cycle; the corresponding $K^+$ diffusion coefficient of (b) CTF-0 and (d) CTF-1.

The apparent diffusion coefficient ($D_{app}$) can be calculated through the following equation:

$$D_{app} = \frac{4}{\pi\tau}\left(\frac{m_B V_M}{M_B}\right)^2\left(\frac{\Delta E_s}{\Delta E_\tau}\right)^2 \quad \left(\tau \ll \frac{L^2}{D}\right)$$

$\tau$ is the time for the galvanostatic charge and discharge process; $V_M$, $M_B$ and $m_B$ are the molar volume, the molecular weight and the mass of active material, respectively. S is the surface area of the electrode. L is the average radius of the active material. $\Delta E_s$ and $\Delta E_\tau$ are steady-state voltage and the total change of the cell voltage during the pulse current. The calculated average apparent diffusion coefficient $\overline{D}$ according to **Figure S7b** and **Figure S7d** are $1.01 \times 10^{-11}$ for CTF-0 and $9.21 \times 10^{-12}$ for CTF-1.

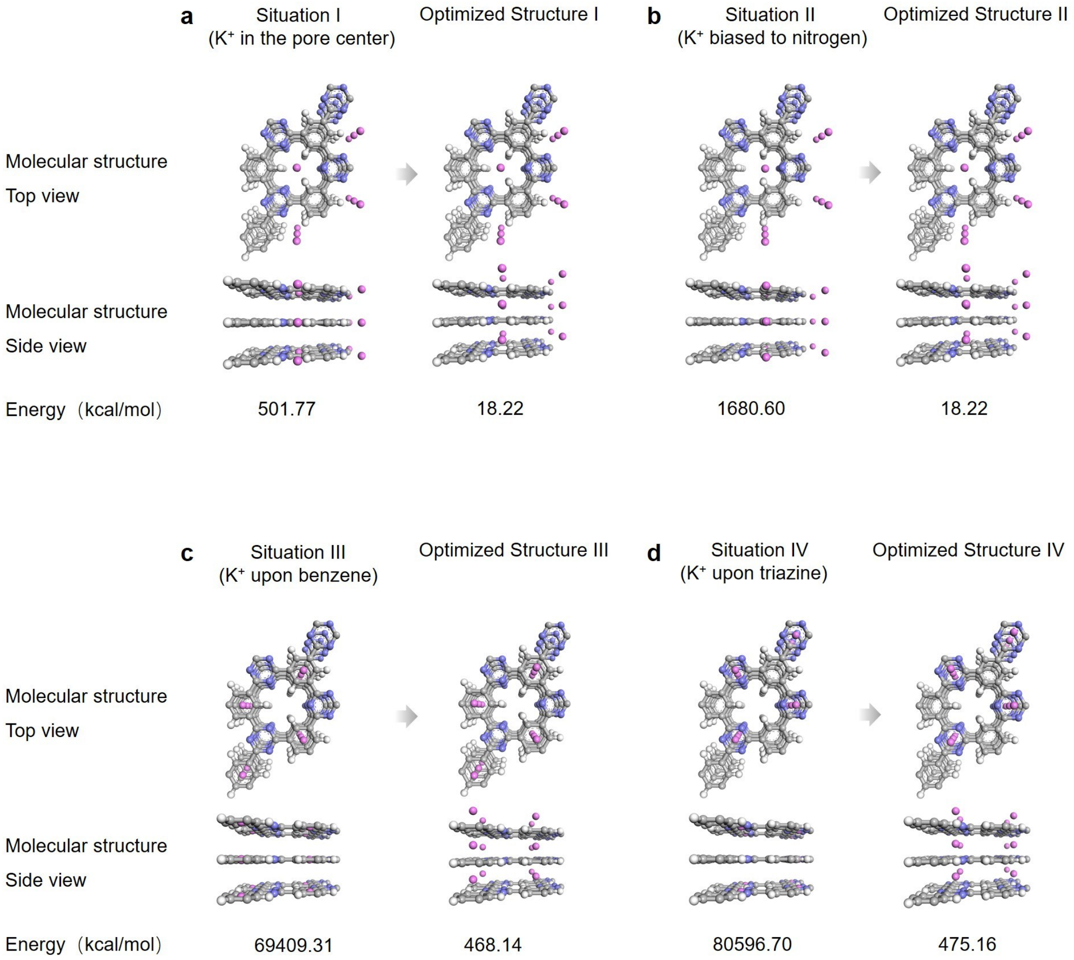

**Figure S8.** Simulated molecular structure for the possible $K^+$ locations in the CTF-0 interlayers. Assembly energies are listed below the corresponding structures. (a) $K^+$ resides in the center of the channel; (b) $K^+$ is biased to the nitrogen of triazine in the channel; (c) $K^+$ is upon the benzene in CTF-0; (d) $K^+$ is upon the triazine in CTF-0. The simulated results demonstrate that the optimized structure I and optimized structure II possess the same structural features and are the most thermodynamically stable structures due to the lowest assembly energies.

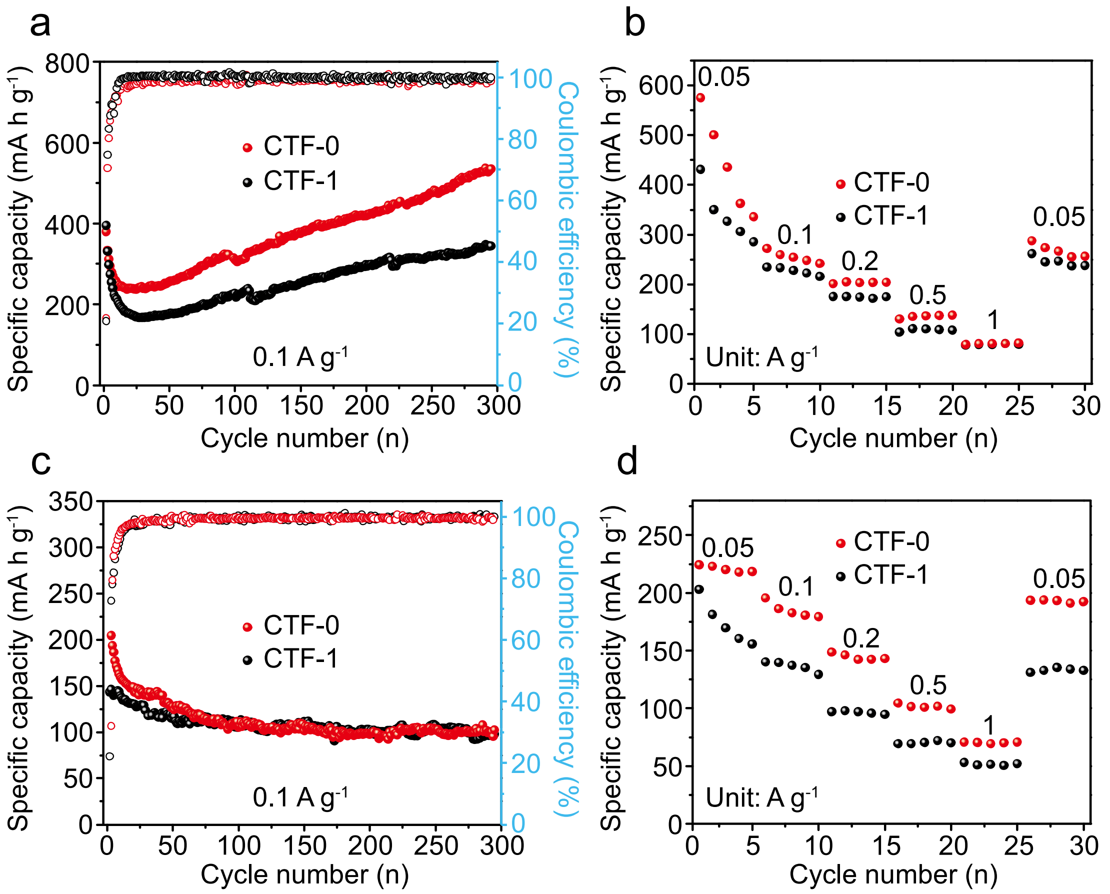

**Figure S9**. (a) The cycling and (b) rate performance of CTFs as anodes for Li-ion batteries. (c) The cycling and (d) rate performance of CTFs as anodes for Na-ion batteries.

**Table S3.** Electrochemical performance comparison between CTFs and previously-reported organic materials when served as anodes for K-ion batteries.

| Organic materials | CTF-0 | CTF-1 | ADAPTS | $K_2TP$ | $K_2BPDC$ @GR | $K_2SBDC$ @GR | $H_2TP$ |
|---|---|---|---|---|---|---|---|
| Retained reversible capacity (mAh $g^{-1}$) / cycle number | 113/200 | 60/200 | 51/1000 | 229/100 | 170/100 | 124/100 | 223/150 |
| Current density (mA $g^{-1}$) | 100 | 100 | 100 | 200 | 50 | 50 | 50 |
| Reference | This work | This work | 1 | 2 | 3 | 3 | 4 |

References:

1. Y. Liang, C. Luo, F. Wang, S. Hou, S.-C. Liou, T. Qing, Q. Li, J. Zheng, C. Cui and C. Wang, *Adv. Energy Mater.*, 2019, **9**, 1802986.
2. K. Lei, F. Li, C. Mu, J. Wang, Q. Zhao, C. Chen and J. Chen, *Energy Environ. Sci.*, 2017, **10**, 552-557.
3. C. Li, Q. Deng, H. Tan, C. Wang, C. Fan, J. Pei, B. Cao, Z. Wang and J. Li, *ACS Appl. Mater. Interfaces*, 2017, **9**, 27414-27420.
4. C. Wang, W. Tang, Z. Yao, Y. Chen, J. Pei and C. Fan, *Org. Electron.*, 2018, **62**, 536-541.

## Experimental methods

### Physical measurements

FTIR spectra (KBr) were recorded on Nicolet IS50 Fourier transforms infrared spectrometer. $N_2$ adsorption isotherms and pore size distributions were obtained at 77K using an Autosorb iQ2 adsorptometer, Quantachrome Instrument. The pore size distribution plot was obtained by applying nonlocal DFT (NLDFT) equilibrium model based on nitrogen adsorption data. PXRD measurements were performed on Rigaku D/MAX2550 diffractometer using Cu-Kα ($\lambda = 1.5418$ Å) radiation running at a voltage of 40 kV and a current of 200 mA. TEM images were measured on JEOL JEM 3010. SEM images were implemented on field emission scanning electron microscope equipped with energy-dispersive X-ray spectroscopy (FE-SEM, SU-8010, Hitachi). The X-ray photoelectron spectroscopy (XPS) spectra were collected on a Thermo ESCALAB 250 instrument using Al-Kα as the exciting radiation (energy step size, 1.0 eV, pass energy, 20.0 eV) and binding energy calibration was based on C 1s at 284.6 eV. Metal contents in COF matrix were measured by inductively coupled plasma mass spectrometry (ICP-MS) on a ThermoScientificiCAP6300. The Thermo Gravimetric Analysis (TGA) experiments were conducted on the Perkin Elmer thermogravimetric analyzer at a heating rate of 10 °C $min^{-1}$ in air condition.

### Molecular simulations

Molecular simulations were carried out by Material Studio 8.0 software using the COMPASS force field implemented in the forcite module. According to the powder diffraction pattern of CTFs, the interlayer distance was derived. After atoms were introduced into the structural unit cell, geometry optimization was performed so as to obtain the optimal periodicities. The resulting hexagonal unit cell parameters for CTF-0 is a, b = 7.3 Å and c = 3.4 Å, while it is a, b = 14.6 Å and c = 3.4 Å for CTF-1. After the geometrical energy minimization, simulated energies for CTFs and $K^+$ incorporated CTFs were obtained.

### Synthesis of CTFs

All staring solid materials and solvents were obtained commercially and used without further purification. CTFs was synthesized following the previous literature[1, 2]. In a typical experiment, a mixture of 1,3,5-tricyanobenzene (*p*-dicyanobenzene) and desiccated $ZnCl_2$ was heated to 400 °C for 40 h in a flame-sealed quartz ampule under vacuum to fabricate the CTF-0 (CTF-1). After cooling to room temperature, the resultant powder was ground thoroughly and washed with water and 0.1 M HCl under vigorous stirring. Finally, the obtained product was successively washed with water, DMSO, and acetone for several times and dried in a vacuum oven at 150 °C for 12 h.

**Electrochemical experiments**

The anode slurry made by mixing 70 wt% active materials (CTF-0 or CTF-1), 20 wt% acetylene black (Sigma Aldrich), 10wt% carboxymethyl cellulose sodium (CMC) binder in deionized water casted on an copper foil and then dried at 60 °C for 12 hours in vacuum. The loading density of the anode active material was around 1.0 mg $cm^{-2}$. The metallic K (purchased from the Aladdin) was used as both the anode and reference electrode. The batteries were assembled by using the CR2032 coin-type cells and glass fiber (Whatman 934-AH (1827-866)) as the separator in the glove box with Ar atmosphere (water content < 0.1 ppm, oxygen content < 0.1 ppm). The electrolyte was 0.8 $mol{\cdot}L^{-1}$ $KPF_6$ in a mixed solvent of EC/DEC (1:1 vol%, purchased from the DoDoChem). Galvanostatic charge-discharge (GCD) was performed using an LAND CT2001A system at 25 °C at various current density with the potential window of 0.01-3.0 V. Cyclic voltammetry (CV) measurements were conducted on a CHI750e electrochemical station. The electrochemical impedance spectroscopy (EIS) tests were measured at a VersaSATA 3 (Princeton Applied Research) electrochemical station (frequency range 0.1-$10^5$ Hz, amplitude 5mV). The Galvanostatic intermittent titration technique (GITT) tests were conducted using the Arbin-BT2000 and the current pulse of 50 mA $g^{-1}$ was used for 12 min, followed by a rest of 4 h.

## Reference

1. P. Katekomol, J. Roeser, M. Bojdys, J. Weber and A. Thomas, *Chem. Mater.*, 2013, **25**, 1542-1548.
2. P. Kuhn, M. Antonietti and A. Thomas, *Angew. Chem. Int. Ed.*, 2008, **47**, 3450-3453.